RESEARCH ARTICLE

JOURNAL OF
Neuroscience Research

Comparison of the effects of two therapeutic strategies based on olfactory ensheathing cell transplantation and repetitive magnetic stimulation after spinal cord injury in female mice

Quentin Delarue[1,2] | Amandine Robac[1,2] | Romane Massardier[1,2] | Jean-Paul Marie[1,2] | Nicolas Guérout[1,2] (iD)

[1]Normandie Univ, UNIROUEN, EA3830-GRHV, Rouen, France

[2]Institute for Research and Innovation in Biomedicine (IRIB), Rouen, France

Correspondence
Quentin Delarue and Nicolas Guérout, Normandie Univ, UNIROUEN, EA3830-GRHV, 76000 Rouen, France.
Email: quentin.delarue@univ-rouen.fr (Q. D.) and nicolas.guerout@univ-rouen.fr (N. G.)

Abstract

Spinal cord injury (SCI) is a debilitating condition, which leads to a permanent loss of functions below the injury site. The events which take place after SCI are characterized by cellular death, release of inhibitory factors, and inflammation. Many therapies have been studied to cure SCI, among them magnetic stimulation aims to reduce the secondary damages in particular by decreasing apoptosis, while, cellular transplantation promotes neuroregeneration by enhancing axonal regrowth. In the present study, we compared individually primary olfactory ensheathing cell (OEC) transplantation and repetitive trans-spinal magnetic stimulation (rTSMS) and then, we combined these two therapeutic approaches on tissue repair and functional recovery after SCI. To do so, SCIs were performed at Th10 level on female C57BL/6 mice, which were randomized into four groups: SCI, SCI + primary bOECs, SCI + STM, SCI + primary bulbar olfactory ensheathing cells (bOECs) + stimulation (STM). On these animals bioluminescence, immunohistological, and behavioral experiments were performed after SCI. Our results show that rTSMS has beneficial effect on the modulation of spinal scar by reducing fibrosis, demyelination, and microglial cell activation and by increasing the astroglial component of the scar, while, primary bOEC transplantation decreases microglial reactivity. At the opposite, locotronic experiments show that both treatments induce functional recovery. We did not observed any additional effect by combining the two therapeutic approaches. Taken together, the present study indicates that primary bOEC transplantation and rTSMS treatment act through different mechanisms after SCI to induce functional recovery. In our experimental paradigm, the combination of the two therapies does not induce any additional benefit.

KEYWORDS
glial scar, magnetic stimulation, olfactory ensheathing cells and neuroregeneration, rehabilitation, RRID:AB_10563302: PDGFRβ, Abcam, ab91066, RRID:AB_10643424: PE,

Amandine Robac and Romane Massardier contributed equally to this work.

poly4064, BioLegend, 406408, RRID:AB_2313568: Jackson ImmunoResearch, 711-166-152, RRID:AB_2340667: Jackson ImmunoResearch, 712-165-153, RRID:AB_2340812: Jackson ImmunoResearch, 715-165-140, RRID:AB_2715913: Alexa 488, MRG2b-85, BioLegend, RRID:AB_306827: p75, Abcam, ab8874, RRID:AB_476889: GFAP Cy3-conjugated Sigma-Aldrich, C9205, RRID:AB_777165:P DGFRβAbcam ab32570, RRID:AB_839504: Iba1, Wako, 019-19741, RRID:AB_94975: MBP, Millipore, MAB386, RRID:IMSR_JAX:008450: L2G85Chco+/+ (FVB-Tg(CAG-luc,-GFP)L2G85Chco/J), spinal cord injury

Significance

Olfactory ensheathing cell (OEC) transplantation and repetitive magnetic stimulation are two distinct promising therapies, which induce tissue repair and functional recovery after spinal cord injury (SCI). However, the comparison between these two therapeutic approaches and the effects of their combination are not known. In our study, we report that rMS has beneficial effect on the modulation of the scar whereas bOEC transplantation decreases inflammation and both treatments enhance functional recovery. Our results demonstrate also that the combination of these two therapies has no additional effect. Altogether, we hypothesize that these two treatments promote recovery after SCI by different mechanisms.

1 | INTRODUCTION

Spinal cord injury (SCI) is an incurable disease, which leads to a permanent loss of motor, and sensitive functions below the injury site (Ahuja et al., 2020). Indeed, SCI induces an interruption of the afferent and efferent pathways due to the disruption of axonal tracts. However, recently, several approaches have been described as able to enhance recovery after SCI. Indeed, we can cite the complex strategy used by Tabakow et al., based on olfactory ensheathing cell (OEC) transplantation with peripheral nerve bridging or the development of new technology using innovative implanted pulse generator which, in both cases, have demonstrated impressive functional results when applied to paraplegic patients (Tabakow et al., 2014; Wagner et al., 2018). Unfortunately, despite these promising results, to date no cure can be offered to the vast majority of injured patients.

Right after the initial physical damages, a cascade of secondary events take place into the lesioned spine (Grégoire et al., 2015; Stenudd et al., 2015). These secondary events begin by the disruption of axons and the release of myelin debris which induce inflammation by the activation of the resident microglial cells and the infiltration of the blood-derived immune cells (O'Shea et al., 2017). Then, resident astrocytes become hypertrophic and overexpress GFAP. At the same time, ependymal cells which are the spinal cord stem cells, proliferate, migrate into the parenchyma, and differentiate into astrocytes; in the same way, type A pericytes give rise to stromal cells (Göritz et al., 2011; Meletis et al., 2008). All these cellular events lead to scar formation. This scar, initially described as a glial scar, is composed of several cellular types which play a dual inhibitory/permissive role (Anderson et al., 2016; Sabelström et al., 2013). Indeed, the scar is composed of astrocytes from two

origins, resident astrocytes and ependymal cells which constitute the glial component of the scar and stromal cells derived from pericytes which constitute the fibrotic component of it. It has been described that, mainly, the fibrotic scar plays an inhibitory role whereas the glial scar constitutes a permissive environment which enhances axonal regrowth (Anderson et al., 2016; Dias et al., 2018). These precise cellular events have been described using different transgenic mouse lines, it is important to note that the processes which take place after SCI in the other mammals such as rats or Humans are not so well described and can differ from one species to another.

Thereby, two different approaches have been proposed as treatment after SCI. The main purpose of the first approach is looking for reducing the secondary damages which take place after SCI; such as neuronal and oligodendroglial death, axonal dieback or release of myelin debris (Abbaszadeh et al., 2020). Several treatments have been tested, among them chondroitinase ABC and anti-Nogo-A are very promising therapies which have been applied with success in both Humans and rodents (Kucher et al., 2018; Muir et al., 2019; Schneider et al., 2019).

The second approach is based on promoting neuroregeneration by enhancing axonal regrowth or replacing lost cells (Ahuja et al., 2020). Indeed, based on several experimental paradigms, studies have reported that functional recoveries can be promoted after SCI in rodents by using neurotrophic factors infusion, cell transplantation, peripheral nerve graft, or combination of different treatments (Decherchi et al., 1997; Kanno et al., 2014; Thornton et al., 2018). In Humans this second approach is mainly based on cell transplantation. Thereby, several trials have been already conducted using autologous stem or differentiated cells (Ahuja et al., 2020; Badner et al., 2017).

Especially, we and others, have demonstrated that OEC transplantation based therapy can promote, in rodent models, functional recovery, and axonal regrowth (Delarue et al., 2020; Khankan et al., 2016; Mayeur et al., 2013).

Recently, a new strategy has emerged, based on the modulation of the spinal scar which takes place after SCI. As we described above, mainly two populations of cells constitute the spinal scar after SCI in mice; astrocytes and fibroblasts (Dias et al., 2018; Göritz et al., 2011). In taking advantage of optogenetic stimulations in transgenic mouse lines, it has been described, that modulation of these cellular populations in particular, by reducing the fibrotic component of the scar can induce axonal regrowth and enhance functional recovery (Dias et al., 2018). These results are a proof of principle that the cellular populations which compose the spinal scar per se can be modulated and not only the molecular components of it.

Newly, we have described that the spinal scar can be modulated using a focal and non-invasive repetitive trans-spinal magnetic stimulation (rTSMS) paradigm (Chalfouh et al., 2020). Indeed, when applied during 14 consecutive days, rTSMS treatment decreases fibrosis and enhances functional recovery (Chalfouh et al., 2020). In our study, we show that rTSMS decreases fibrosis and increases astroglial scar by enhancing ependymal cells' proliferation and their contribution to the scar by their differentiation into astrocytes and oligodendrocytes. Moreover, rTSMS decreases apoptosis which leads to neuronal survival and axonal regrowth (Chalfouh et al., 2020).

Altogether, it appears that cell transplantation and magnetic stimulation can promote recovery after SCI by different cellular and molecular mechanisms. A recent study have compared and combined several strategies based on stem cell transplantation and repetitive transcranial magnetic stimulation in rats (Guo et al., 2020). However, to our knowledge, our study is the first one to compare and combine rTSMS and OEC transplantation after SCI. That is why we propose here to compare and combine these two therapies in a severe SCI model in mice.

2 | MATERIALS AND METHODS

2.1 | Animal care and use statement

The animal protocol was designed to minimize pain or discomfort to the animals. All experimental procedures were in accordance with the European Community guiding principles on the care and use of animals (86/609/CEE; Official Journal of the European Communities no. L358; December 18, 1986), French Decree no. 97/748 of October 19, 1987 (Journal Officiel de la République Française; October 20, 1987), and the recommendations of the Cenomexa ethics committee (#20458).

2.2 | Animals

Female mice group housed (two to five mice/cage) in secure conventional rodent facilities on a 12-hr light/dark cycle with constant access to food and water.

A total of 54 mice were included in this study (Figure 1). We used two mouse lines in this study (48 wild type (WT) C57BL/6 mice and 6 Tg (CAG-luc,-GFP) L2G85Chco$^{+/+}$ (FVB-Tg(CAG-luc,-GFP) L2G85Chco/J,) mice called Luciferase (LUX) thereafter. LUX mice were obtained from the Jackson Laboratory (https://www.jax.org/strain/008450, RRID:IMSR_JAX:008450). Then, LUX mice have been crossed with C57BL/6 mice three times consecutively to be sure to avoid any problem related to the strains.
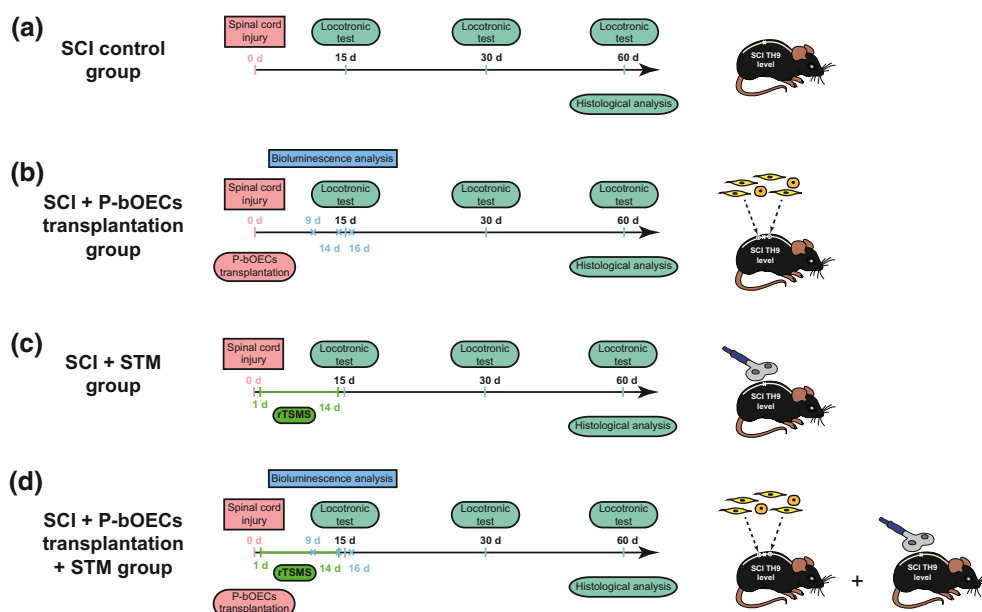
FIGURE 1 Experimental paradigm illustrating the timeline of the major experimental manipulations [Color figure can be viewed at wileyonlinelibrary.com]

Eight WT mice have been used to characterize the primary bOECs cultures.

Our study was composed of four main experimental groups:

SCI control group: animals received spinal cord injury ($N = 10$).

SCI + bOEC group: animals received spinal cord injury and primary bOEC transplantation ($N = 10$).

SCI + STM group: animals received spinal cord injury and rTSMS treatment during 14 days ($N = 10$).

SCI + bOECs + STM group: animals received spinal cord injury and primary bOEC transplantation and rTSMS treatment during 14 days ($N = 10$).

Transplanted primary bOECs was obtained from LUX $\pm$ mice ($n = 6$).

An overview of the paradigms used in this study is presented in Figure 1.

All the experiments were carried out and distributed between three different researchers. SCI, primary OB cultures, and transplantations have been performed by one researcher who performed also histological experiments and statistical analysis, whereas magnetic stimulation, bioluminescence, and locotronic experiments have been performed independently by two other researchers.

2.3 | Primary olfactory bulb culture and cell transplant preparation

Olfactory bulb (OB) primary cultures were prepared as described previously (Delarue et al., 2020; Guérout et al., 2010). Briefly, after anesthesia with 2% of isofluorane (Iso-Vet, Osalia, Paris, France), mice were euthanized by decapitation and OBs were removed from the brain and put in cold PBS. The tissue were dissociated first by trypsinization 0.25% (2.5% Trypsin 10X, 15090-046, Thermofisher) and then mechanically. After dissociation cells were cultured in T25 flask with 5 ml of DF-10S media. DF10s was reconstituted with DMEM:F12 + glutamax, 0.5% Penicillin/Streptomycin, and 10% heat-inactivated fetal bovine serum (30 min at 56°C). Three weeks after plating, cultures were trypsinized, and the cells were counted. Before transplantations, bOECs were resuspended in DF-10S at concentration of 25.000 cells/μL.

2.4 | Flow cytometry and bOEC characterization

Cells were characterized by flow cytometry 3 weeks after plating ($n = 8$ WT mice). For analysis, the number of primary bOECs were adjusted to a density of $2x10^5$ cells/ml in phosphate-buffered saline (PBS)/bovine serum albumin (BSA) solution. TruStain FcX™ PLUS (BioLegend) was added to block non-specific binding. Characterization was performed using rabbit anti-p75 nerve growth factor receptor (p75, Abcam, ab8874, RRID:AB_306827) and rat anti-platelet-derived growth factor β (PDGFRβ, Abcam, ab91066, RRID:AB_10563302) primary antibodies. P75 positive (with a p75high or a p75low expression) and PDGFRβ negative cells were defined as OECs. PDGFRβ positive and P75 negative cells were identified as stromal cells. Primary antibodies were revealed with the anti-rabbit phycoerythrin fluorochrome-conjugated (PE, poly4064, BioLegend, 406408, RRID:AB_10643424) and the anti-rat Aexafluor 488 fluorochrome-conjugated antibodies (AF488, MRG2b-85, BioLegend, RRID:AB_2715913). Data were analyzed using FlowJo software (version 10.3; FlowJo LLC).

2.5 | Surgical procedure and cell transplantation

Mice received 30 min before surgery an intramuscular injection of nalbuphine hydrochloride (10 mg/ml, Mylan, Canonsburg, PA). Then, mice were anesthetized with 2% of isofluorane during the entire surgery (Iso-Vet, Osalia, Paris, France). Animal's body temperature has been kept steady at 37°C with a heating pad during entire surgical intervention. SCI were performed at T10 level as described previously (Li et al., 2016). After being shaved and disinfected with 70% EtOH, the dorsal skin of the mice was incised, the superficial fat gently shifted, and the muscle tissue dissected to expose laminae T9–T11. Posterior part of vertebrae was countersank in order to create an ample space for lesion. After laminectomy, the dura mater was removed and a complete transection of the spinal cord was performed with 25-gauge needle, right after the lesion, bOECs were transplanted (Figure 1). To facilitate cells transplantation, a stereotaxic frame with its micromanipulator arm (World Precision Instrument) was used. Thus, primary bOECs were injected using a 1-mm sterile glass capillary needle, which was attached to the micromanipulator. Injections were delivered at 0.6 mm depth, 0.4 mm from the midline at the left, 5 mm rostrally, and caudally from the lesion site. A total of two injections (2×2 μl), which contained 25.000 cells/μl, was delivered. Each injectate was carefully delivered within 1 min.

After surgery, mice underwent daily check, none of them showed neither skin lesion, infection, nor autophagy throughout the study.

2.6 | Bioluminescence imaging

An *in vivo* XTREM 4XP spectrum cooled charge-coupled device optical macroscopic imaging system (Brucker) was used for bioimaging. The survival of the LUX$^{+/-}$ primary bOECs was monitored during 2.5 weeks via intraperitoneal injections of D-Luciferin (0.3 mg/g body weight) at 9, 14, and 16 days after SCI and measurements of the photon counts were performed as previously described using Brucker molecular imaging software (Delarue et al., 2020).

2.7 | rTSMS treatment

rTSMS was delivered with a commercially available figure of eight double coil featuring an air cooling system connected to a Magstim

rapid[2] stimulator used for focal cortical and peripheral stimulations (Magstim, Whitland, UK). The coil was positioned in close contact with the back of the animal at the site of injury. The size of the area stimulated has been defined according to manufacturer's device manual. The area stimulated was 1.5cm[2]. The position of the coil was maintained using an articulated arm stand. The exact position of the coil was defined using the mark located in the middle of the coil.

rTSMS treatment was applied at a frequency of 10Hz, 10 min per day during 14 days, the day after SCI (Figure 1). Stimulation protocol consisted of 10s stimulation followed by 20s of rest. Mice were kept anesthetized with 2% of isoflurane during stimulation, the equivalent anesthesia were used for untreated animals. Peak magnetic intensity at the experimental distance was 0.4T.

2.8 | Tissue preparation and sectioning

Animals were deeply anesthetized with sodium pentobarbital (150 mg/kg body weight) and perfused transcardially with PBS followed by ice-cold 4% formaldehyde in PBS. Dissected spinal cords were further post-fixed in 4% PFA in PBS at 4°C overnight and cryoprotected in 30% sucrose (Life Technologies, Carlsbad, CA) for at least 48 hr. After embedding in Tissue-Tek OCT compound (Sakura, Tokyo, Japan), the spinal cords were cut sagittally to 20 μm thickness. Sections were collected accordingly to stereological principles (five sections per slide for sagittal sections) and stored at − 20°C until further use.

2.9 | Immunohistochemistry

Spinal cord sections were blocked with 10% normal donkey serum (Jackson ImmunoResearch, Cambridge, UK), 0.3% Triton-X100 (Sigma-Aldrich) in PBS, then incubated overnight at room temperature in a humidified chamber with primary antibodies diluted in blocking solution. The following primary antibodies were used: Rabbit anti-platelet-derived growth factor β (PDGFRβ, Abcam, ab32570, RRID:AB_777165), mouse anti-glial fibrillary acidic protein (GFAP Cy3-conjugated Sigma-Aldrich, C9205, RRID:AB_476889), rabbit anti-ionized calcium-binding adapter molecule 1 (Iba1, Wako, 019-19741, Osaka, Japan, RRID:AB_839504), and rat anti-myelin basic protein (MBP, Millipore, MAB386, RRID:AB_94975).

After washing, antibody staining was revealed using species-specific fluorescence-conjugated secondary antibodies (Jackson ImmunoResearch, 711-166-152, RRID:AB_2313568, 715-165-140, RRID:AB_2340812, 712-165-153, RRID:AB_2340667). Sections were counterstained with 4',6-diamidino-2-phénylindole (DAPI; 1 μg/ml; Sigma-Aldrich) and coverslipped with Vectashield mounting media (Vector Labs, Burlingame, UK).

2.10 | Image acquisition analysis

Representative images of the lesion site were acquired using the Zeiss Apotome2 microscope set up at 60 days after SCI. For tissue analysis sagittal sections have been used. For each experimental group and staining, five animals were analyzed. The cross section of spinal cord showing the epicenter of the lesion was taken and analyzed for each animal. The image processing and assembly were acquired with Image J software.

2.11 | Quantification of immunohistochemically stained areas

Three to five sections per animal were observed in order to determine the epicenter of the lesion. Then, an image of the epicenter was taken and analyzed. On these sagittal sections, the GFAP-, PDGFrβ+, and MBP- areas were measured. To standardize Iba1 measurement, analysis of intensity was performed on rectangle of 6 μm × 2 μm. Iba1 intensities were collected after threshold standardization.

## 2.12 | Locotronic test: Foot misplacement apparatus

Experiments have been performed as described previously by Chort et al. (Intellibio, Nancy, France) (Chort et al., 2013). The equipment consists of a flat ladder on which the animal can move from the starting zone toward the arrival zone. On both sides of the ladder, infrared sensors allow the visualization and recording of the displacement of the animal. The location and precise length of time of all the errors are recorded, in distinguishing the errors from front legs, back legs, and tail. Based on all data recorded; number of back leg errors, total back leg error time, and total crossing time were provided by the software and compared between groups of animals.

All the mice were pre-trained on the ladder, twice, 1 week prior to injury and then assessed the day before the surgery to provide baseline data. Experiment were performed three times 15, 30, and 60 days after SCI.

2.13 | Statistical analysis

2.13.1 | Statistical analyses have been carried out blindly

All data are presented as means ± standard deviation (*SD*). Shapiro tests were performed for assessing data distribution. These tests reveal that our data are not normally distributed. That is why nonparametric tests have been performed. Comparison of means were
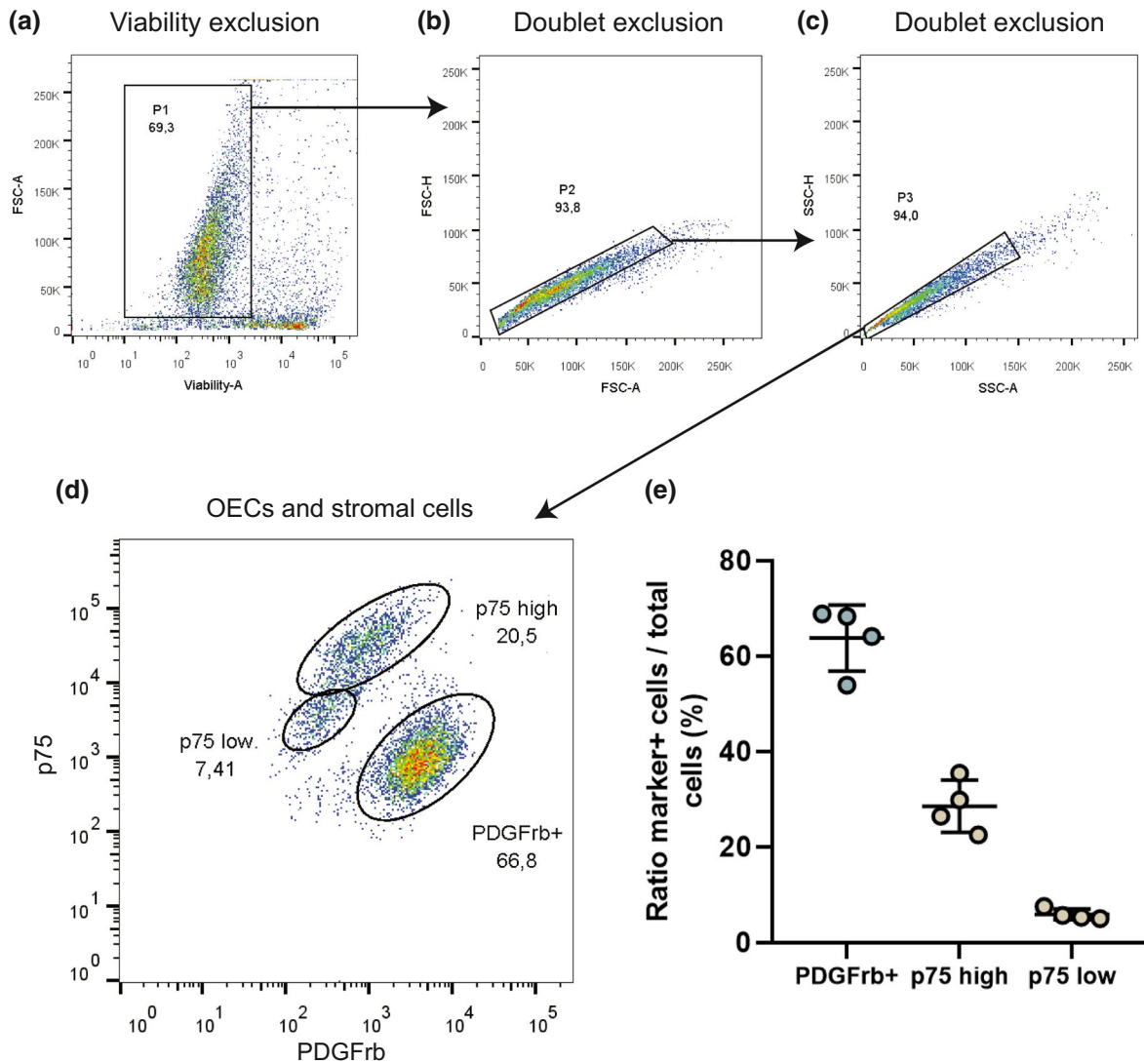
FIGURE 2 Cellular characterization of bOEC primary culture by flow cytometry. Cells are isolated after (a) viability exclusion and (b and c) doublet exclusion. (d) Cells are characterized using anti-p75 and anti-PDGFrβ antibodies. Olfactory ensheating cells (OECs) were defined as p75high or p75low positive and PDGFrβ negative cells. Stromal cell was defined as PDGFrβ positive (PDGFrβ+) and p75 negative cells. (e) Cell ratio in the bOEC primary culture. Dot plots represent mean ± standard deviation. $N = 4$ per group. All experiments were conducted in duplicate [Color figure can be viewed at wileyonlinelibrary.com]

performed using Mann–Whitney test for Figure 3. Comparison of medians was performed using Kruskal–Wallis tests for Figures 4–6. In all tests, $p < 0.05$ were considered statically significant.

3 | RESULTS

3.1 | Characterization of the two cell populations in primary bOEC cultures

To determine the cell populations present in the primary OB cultures, flow cytometry analyses were performed. After viability exclusion (Figure 2a) and two doublet exclusions (Figure 2b,c), flow cytometry revealed that primary bOEC cultures contain two distinct populations of cells; fibroblasts (PDGFrβ positive cells) and OECs

(p75 positive cells). In effect, in these cultures, 63.8% ± 6.9% of the cells were PDGFrβ positive and 34.4% ± 6.4% cells were p75 positive. The p75 population was in fact, as previously described by our laboratory in rats (Honoré et al., 2012), composed of two subpopulations, one which expresses low level of p75 (5.9% ± 1.1%) called p75 low and one which expresses high level of p75 (28.5% ± 5.5%), called p75 high (Figure 2d,e).

3.2 | The survival of transplanted primary bOECs is not influenced by rTSMS treatment

Before to compare the effects of the two therapies and there combined effects on functional recovery and tissue repair, we analyzed the impact of rTSMS treatment on the survival of transplanted
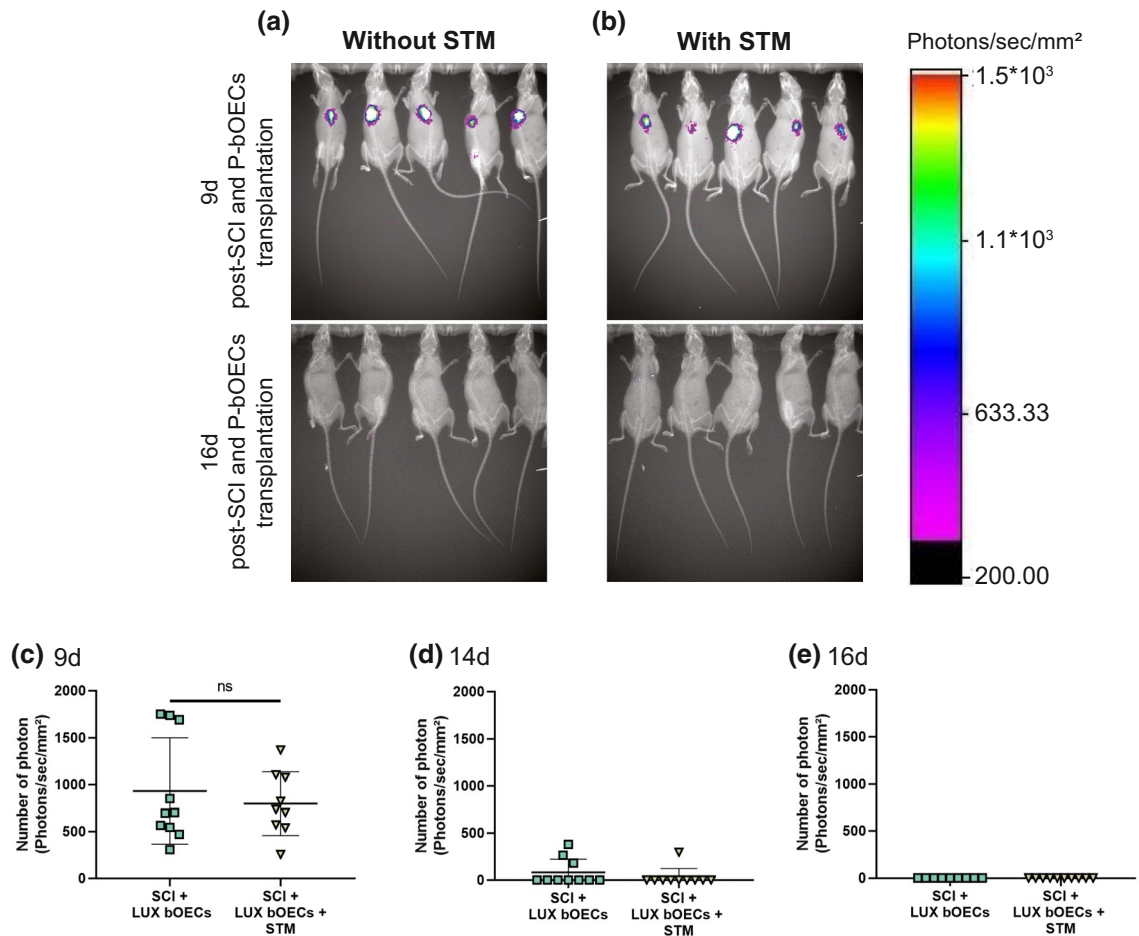
FIGURE 3 The survival of transplanted primary bOECs is not influenced by rTSMS treatment. (a and b) Representative images of luciferase+ (LUX) primary bOECs transplanted in mice stimulated or not at 9d and 16d after SCI. (c–e) Quantification of luciferase signals at (c) 9d, (d) 14d, and (e) 16d after SCI and/or rTSMS treatment. Quantifications are expressed as average ± standard deviation. $N = 10$ per group. Statistical evaluations were based on Mann–Whitney test (ns = not significant) [Color figure can be viewed at wileyonlinelibrary.com]

primary bOECs. We performed bOECs primary culture with cells obtained from LUX ± mice. Then, using bioluminescence imaging system we followed the transplanted cells overtime. We transplanted the same number of cells (100.10^3 cells) in 20 mice divided in two groups of 10 and in one of it, rTSMS treatment has been applied during 14 consecutive days (Figure 3a,b). By quantification of emitted photons, we measured in each group the number of remaining cells at 9 days, 14 days, and 16 days after SCI (Figure 3c–e). Our data show that there is no significant statistical difference between groups with and without rTSMS treatment. The number of surviving cells was the same in each group 9, 14, and 16 days after SCI. Specifically, surviving cells could be observed in all the mice in both groups of animals at 9 days after SCI (Figure 3c). Fourteen days after SCI, surviving cells could be found in only three mice in bOEC group and in only one mouse in STM group (Figure 3d). Sixteen days after SCI, we could not see any surviving cells in both groups of mice (Figure 3a,b, and e). These results suggest that rTSMS treatment does not affect the survival of the transplanted primary bOECs after SCI.
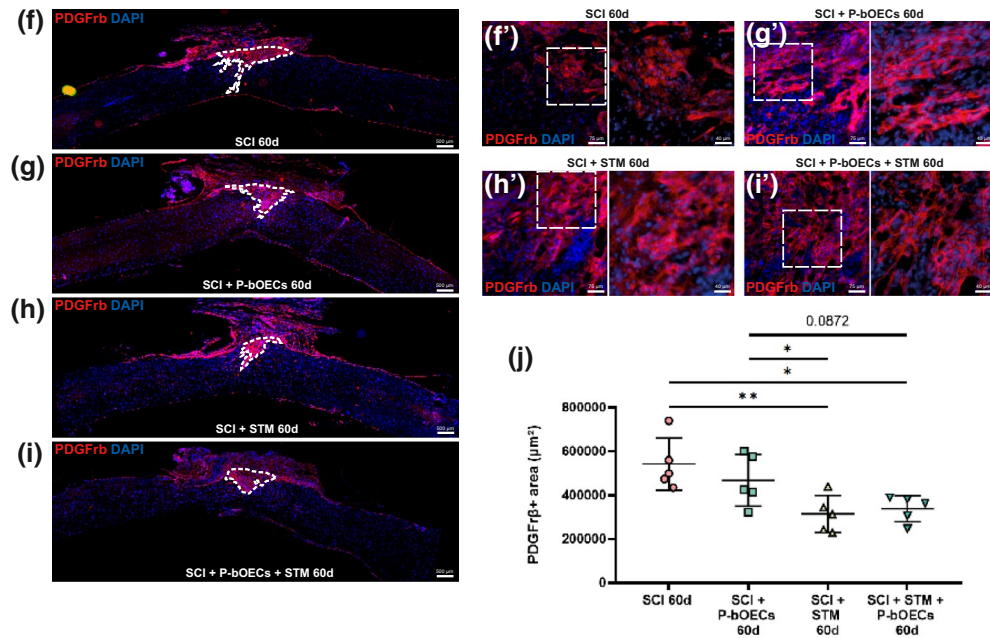
3.3 | rTSMS treatment modulates glial and fibrotic scars but not primary bOEC transplantation

In order to investigate the impact of the two therapies on tissue repair, we performed histological analyses on SCI, SCI + primary bOECs, SCI + STM, and SCI + primary bOECs + STM groups 60 days after SCI. As the scar which takes place after SCI is mainly composed of astrocytes and fibroblasts, we measured the glial scar (Figure 4a–e) and the fibrotic scar (Figure 4f–j) after primary bOEC transplantation, rTSMS treatment, or the combination of the two therapies. To do so, in a first time we analyzed the GFAP negative (GFAP-) area, our results show that in SCI + primary bOEC group (Figure 4b,e) astrocytic scar is not statically different to the SCI control group (Figure 4a,e), whereas at the same time in rTSMS groups (STM and primary bOECs + STM groups), the "astrocyte-free" areas are smaller than in SCI control group (Figure 4c–e). Our results also show that in rTSMS groups (STM and primary bOECs + STM groups) the GFAP negative area is smaller than in bOECs transplanted group (Figure 4c–e).
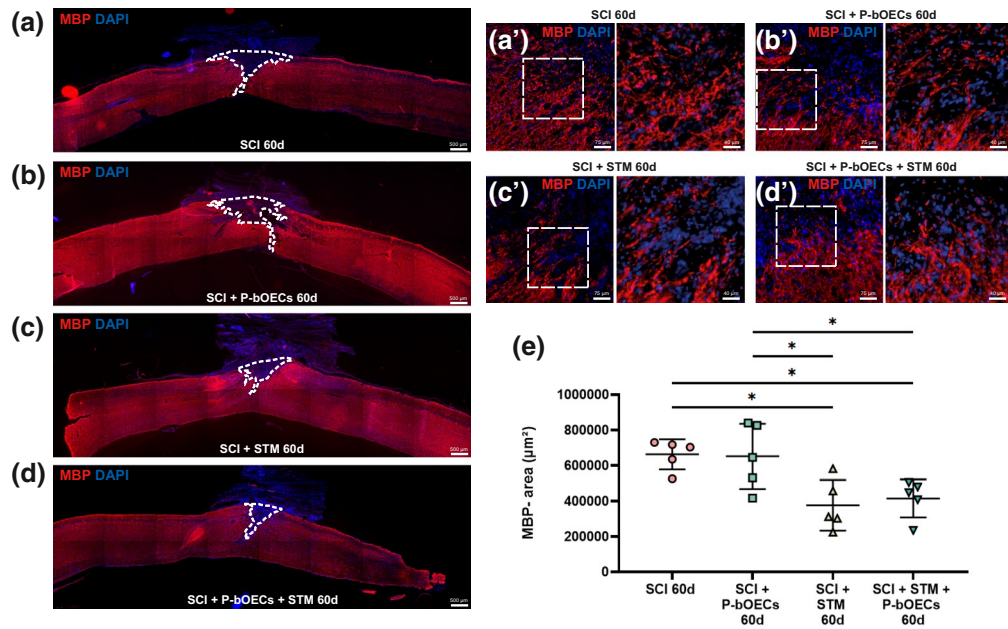
Astrocyte
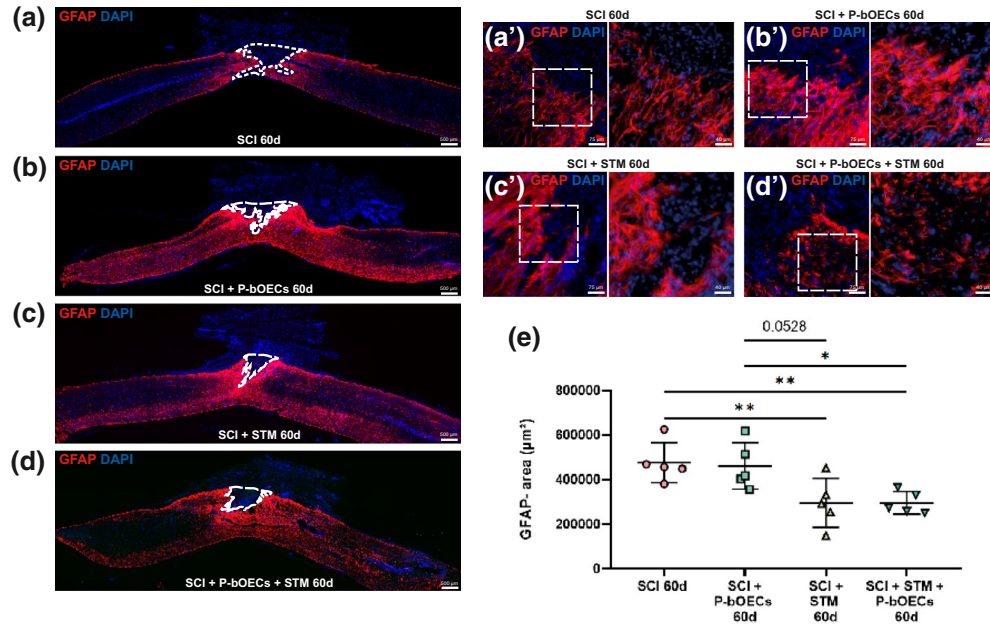
Stromal cell

FIGURE 4 rTSMS treatment modulates glial and fibrotic scars but not primary bOEC transplantation. Representative pictures of sagittal spinal cord sections 60 days after SCI (a, b, c, d, f, g, h, and I 50× magnification) and border of the spinal cord scar (a', b', c', d', f', g', h', and i 200× magnification). (a and f) SCI control, (b and g) SCI + primary bOECs, (c and h) SCI + STM, (d and i) SCI + primary bOECs + STM. Sections were stained with (a–d) anti-GFAP antibody, (f–j) anti-PDGFrβ antibody and DAPI. Dotted lines show (a–d) astrocytic negative area (GFAP-) and (f–i) PDGFrβ positive area (PDGFrβ+). (e and j) Quantitative analysis of (e) GFAP- areas and (j) PDGFrβ + areas. Quantifications are expressed as average ± standard deviation. *N* = 5 per group. Statistical evaluations were based on Kruskal–Wallis test (*$p < 0.05$; **$p < 0.01$) [Color figure can be viewed at wileyonlinelibrary.com]

To complete the scar analysis, in a second time, we quantified the PDGFrβ positive area (PDGFrβ+). In the same way, our results show that the fibrosis component is reduced in SCI + STM (Figure 4h,j) and SCI + primary bOECs + S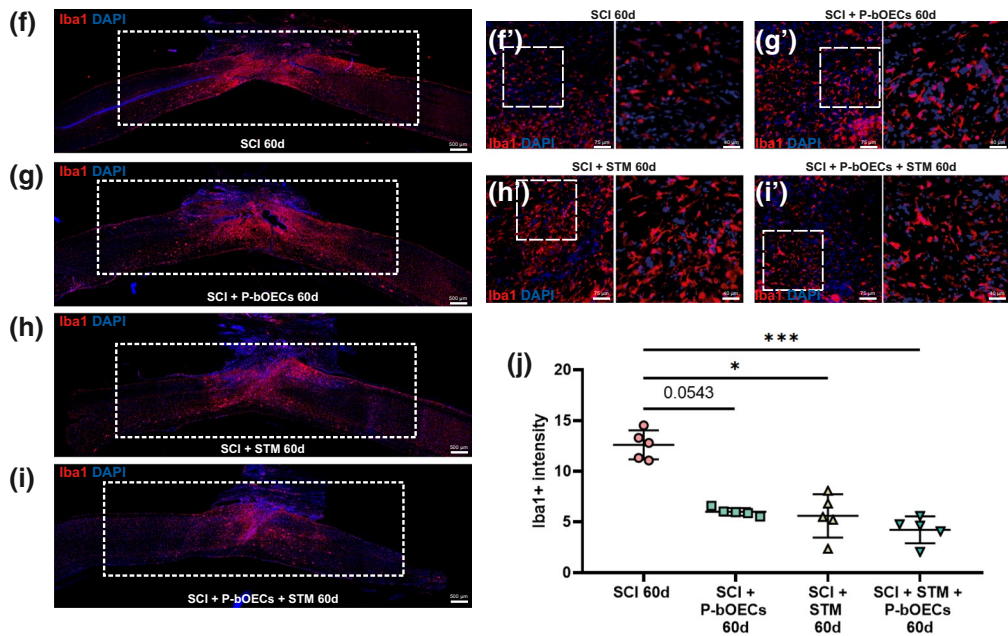TM (Figure 4i,j) groups but not in SCI + primary bOEC group (Figure 4g,j), in comparison to SCI group (Figure 4f,j). It appears that in the rTSMS groups (STM and primary bOECs + STM groups) the PDGFrβ+ areas are smaller than in the transplanted primary bOEC group (Figure 4g–j).

Oligodendrocyte

FIGURE 5 Primary bOEC transplantation and rTSMS treatment decrease microglial cells activation but only rTSMS treatment decreases demyelination. Representative pictures of sagittal spinal cord sections 60 days after SCI (a, b, c, d, f, g, h, and I 50× magnification) and border of the spinal cord scar (a', b', c', d', f', g', h', and i 200× magnification). (a and f) SCI control, (b and g) SCI + primary bOECs, (c and h) SCI + STM, (d and i) SCI + primary bOECs + STM. Sections were stained with (a–d) anti-MBP antibody, (f–j) anti-Iba1 antibody and DAPI. Dotted lines show (a–d) demyelinated area (MBP-). Rectangles show (f–i) Iba1 intensity areas measured. (e and j) Quantitative analysis of (e) MBP- area and (j) Iba1 intensity. Quantifications are expressed as average ± standard deviation. $N = 5$ per group. Statistical evaluations were based on Kruskal–Wallis test (*$p < 0.05$; **$p < 0.01$; ***$p < 0.001$) [Color figure can be viewed at wileyonlinelibrary.com]

Altogether, these results show that only rTSMS treatment has an effect on the modulation of the spinal scar by decreasing fibrosis and increasing astroglial scar.

Cell morphology at the lesion epicenter has been also assessed for astrocytes (Figure 4a'–d') and for stromal cells (Figure 4f'–i'). Our analysis reveals that no change could be observed between groups.
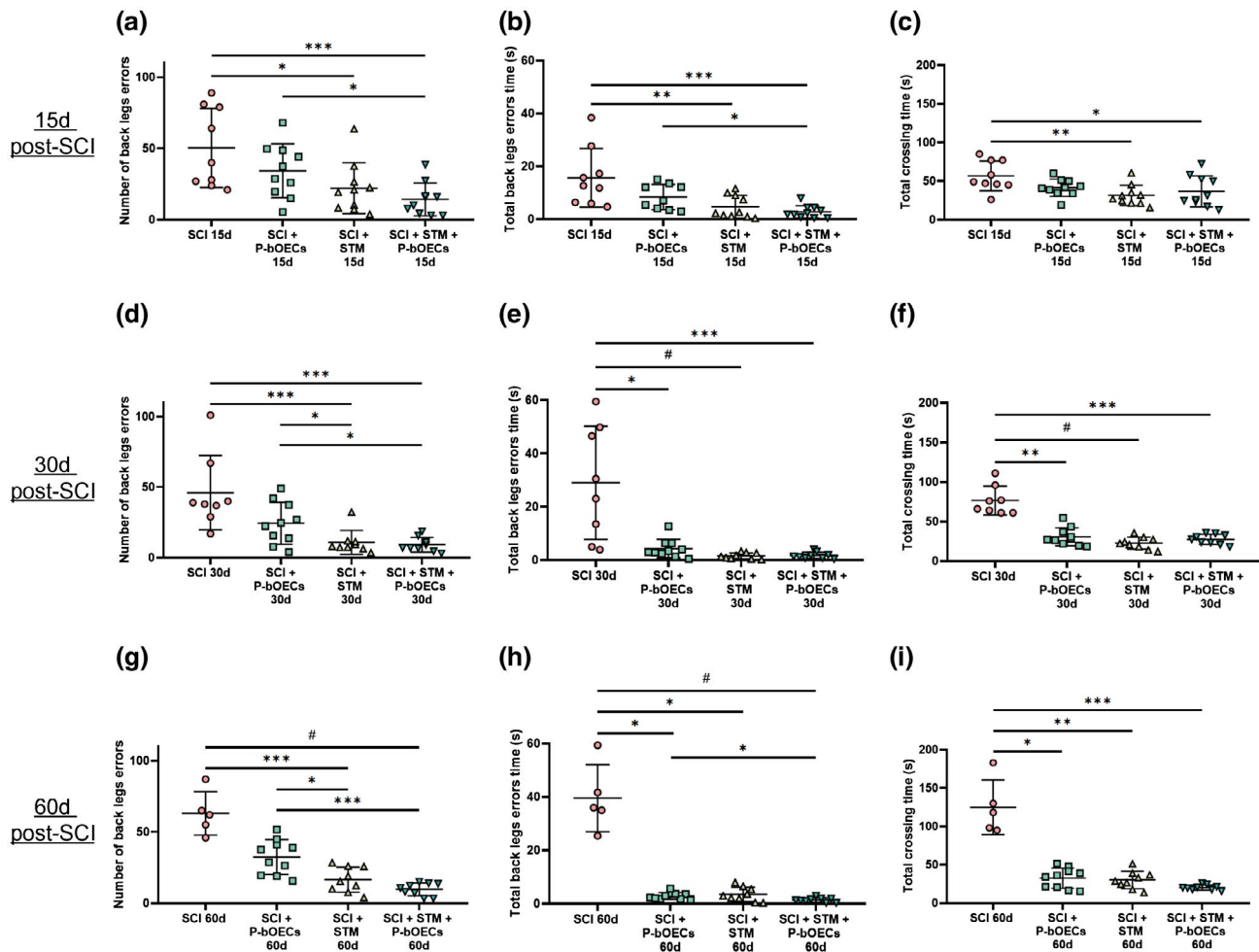
FIGURE 6 Primary bOEC transplantation and rTSMS treatment enhance functional recovery after SCI. Quantification of locotronic evaluation at (a–c) 15 days, (d–f) 30 days, and (g–i) 60 days after SCI. Parameters are (a, d, and g) number of back leg errors, (b, e, and h) total back leg error time and (c, f, and i) total crossing time. Quantifications are expressed as average ± standard deviation. N = 5–10 in control group and N = 8–10 in SCI + primary bOECs, SCI + STM and SCI + primary bOECs + STM groups. Statistical evaluations were based on Kruskal–Wallis test (*p < 0.05; **p < 0.01; ***p < 0.001; #p < 0.0001) [Color figure can be viewed at wileyonlinelibrary.com]

3.4 | Primary bOEC transplantation and rTSMS treatment decrease microglial cell activation but only rTSMS treatment decreases demyelination

To evaluate the therapies' effects on the other spinal cord cell populations, we investigated the myelination/demyelination process and the microglial cell reactivity in the SCI control, primary bOECs, STM, and primary bOECs + STM mice 60 days after SCI. We first analyzed demyelination process by using MBP staining (Figure 5a–e) and by quantification of the MBP negative (MBP-) areas. We found that MBP- area is reduced in SCI + STM (Figure 5c) and SCI + primary bOECs + STM (Figure 5d) groups whereas primary bOECs alone had no effect on this parameter in comparison to the control SCI group (Figure 5a,b,e). Our results demonstrate also that in the rTSMS groups (STM and primary bOECs + STM groups) the MBP negative areas are smaller than in primary bOEC group (Figure 5b–e).

We further investigated the effects of these therapies on microglial cells activation by Iba1 intensity quantification (Figure 5f–j). By quantifying an area of 12 mm^2 including lesion core and the

caudal and rostral parts spaced 3 mm from the epicenter of the lesion, it appears that all therapies (primary bOECs, STM, and primary bOECs + STM groups) decrease microglial cells activation (Figure 5f–j). Our results show that there is no difference between treated groups (Figure 5g–j).

Cell morphology at the lesion epicenter have been also assessed for oligodendrocytes (Figure 5a'–d') and for microglia/macrophage cells (Figure 5f'–i'). Our analysis reveals that no change could be observed between groups.

3.5 | Primary bOEC transplantation and rTSMS treatment enhance functional recovery after SCI

To correlate the beneficial effects of primary bOEC transplantation and rTSMS treatment obtained on tissue repair, with functional recovery, we conducted sensorimotor test. To do so, we used locotronic test which allows to measure three distinct and complementary parameters: the number of back leg errors (Figure 6a,d,g),

the total back leg error time (Figure 6b,e,h), and the total crossing time (Figure 6c,f,i). We performed these tests 15 (Figure 6a–c), 30 (Figure 6d–f), and 60 (Figure 6g–i) days after SCI.

Our results showed that at 15 days post-SCI, only rTSMS-based treatment (STM and primary bOECs + STM groups) improves functional recovery. Indeed, the number of back leg errors, the total back leg error time, and the total crossing time were lower in the two rTSMS groups (STM and primary bOECs + STM groups) in comparison to the SCI control group.

More interestingly, our analysis shows that 30 days after SCI, primary bOEC transplantation alone induced functional recovery compared to the SCI control group, observable by the reduction of the total back leg error time and the total crossing time (Figure 6e,f). As described at 15 days after SCI, it appears also that rTSMS-based treatment (STM and primary OECs + STM groups) induces functional recovery for all the parameters tested (Figure 6d–f).

Lastly, we performed this test at 60 days after SCI, we found the same results as at 30 days after SCI. All therapies (primary bOECs, STM, and primary bOECs + STM) induce functional recovery regarding the total back leg error time and the total crossing time (Figure 6h,i). Only rTSMS-based therapy (STM and primary bOECs + STM groups) showed significant differences in the number of back leg errors (Figure 6g).

Our locotronic test results also show that rTSMS treatment (STM or primary bOECs + STM groups) reduces the number of back leg errors in comparison to the primary bOEC group for all the time points analyzed (Figure 6a,d,g).

4 | DISCUSSION

The main purpose of our study was to compare and combine two therapies, primary bOEC transplantation and rTSMS treatment, after SCI. To do so, three treated groups of mice (1-primary bOECs, 2-rTSMS, and 3-primary bOECs + rTSMS) have been used and compared to untreated mice (SCI group). No control group has been added to the experimental design due to the fact that the main point was to compare the potential benefits obtained after treatment to untreated animals after SCI.

In our study, we demonstrated that both; primary bOEC transplantation and rTSMS treatment can enhance functional recovery after SCI (Figure 6). Our results also show that these two clinically relevant treatments induce their effects by different molecular and cellular mechanisms. Indeed, immunohistological results indicate that only rTSMS treatment modifies the spinal scar by decreasing fibrosis and demyelination and increasing the astroglial component of the scar, whereas bOEC transplantation did not have a strong effect on these parameters (Figures 4 and 5). On the other hand, Iba1 intensity measurement indicates that both therapies reduce activation of microglial/macrophage cells (Figure 5). Finally, our results demonstrate, too, that there is no additional benefit when both therapies are applied together (Figures 4-6). In effect, neither

immunohistological data nor locotronic analyses show differences between STM and primary bOECs + STM groups.

It is very important to note that our histological analyses are based on the measurements of the different areas present at the epicenter of the lesion, which are representative of the different cellular populations which constitute the scar. Indeed, we measured the glial, fibrotic, and myelinated components of the scar based on GFAP, PDGFrβ, and MBP staining, respectively. This method is one of the mostly used nowadays (Chalfouh et al., 2020; Delarue et al., 2020; Li et al., 2016, 2020). However, another method is currently used also, this method is based on intensity measurements, mainly GFAP intensity is assessed in order to evaluate gliosis and hypertrophic astrocytes. Based on GFAP intensity measurement, it has been described that OEC transplantation reduces gliosis after SCI (López-Vales, Forés, Navarro, et al., 2006; López-Vales, Forés, Verdú, et al., 2006; López-Vales et al., 2007; Wang et al., 2021). The fact that two distinct methods have been used to assess tissue repair after SCI and OEC transplantation can explain the differences between our results and some previously published studies where gliosis and hypertrophic astrocytes have been assessed.

In our study, we show that primary bOEC transplantation decreases inflammation. Our results are in agreement with previously published studies. Indeed, Khankan et al, have demonstrated that OEC transplantation facilitates neuroregeneration by modulation of the inflammatory responses (Khankan et al., 2016). More recently, the immunomodulatory role played by OECs after transplantation has been described (Zhang et al., 2021). In particular, in this study the authors show that OECs decrease inflammation at the lesion site *via* interleukin-1 receptor signaling pathway (Zhang et al., 2021).

It is now well described that OECs and in particular bOEC transplantation enhances functional recovery (Li et al., 1997; Watzlawick et al., 2016). In the vast majority of the previously published studies the most commonly used test is the The Basso, Beattie and Bresnahan (BBB) score (Watzlawick et al., 2016). In contrast, in our study neurobehavioral recovery has been assessed using a computer-assisted test; the locotronic test. Our results are in agreement with those published previously by other teams, indeed they demonstrate that primary OEC transplantation induces functional recovery after SCI. In particular, our locotronic results show that primary OEC transplantation enhances locomotion 30 days and 60 days after SCI and transplantation. Interestingly, locotronic test shows that primary bOEC transplantation induces functional recovery but at a later time point than rTSMS treatment. Indeed, rTSMS enhances functional recovery 15 days after SCI whereas we could observe a significant increase of it in primary bOEC group only 30 days after SCI. These data related to "late" recovery are in agreement with our previously published study in rats, in which we showed that OEC transplantation enhances recovery only at 60 days after SCI (Mayeur et al., 2013).

To date, the precise mechanisms by which OECs play their key role during neurogeneration is still poorly described. In fact, OEC transplantation reduces axonal dieback and inflammation at the lesion site (Khankan et al., 2016; Zhang et al., 2021). Moreover, it has been also described that OEC transplantation modulates chondroitin

sulfate proteoglycan (CSPG) expression in injured spinal cord (Wang et al., 2021). Several studies have demonstrated as well that OECs secrete different neurotrophic factors (Blumenthal et al., 2013; Gu et al., 2017; Lipson et al., 2003). Phagocytic properties of OECs may also explain the positive role played by these cells in SCI context. Indeed, it has been described that OECs can phagocyte axon debris during development but also after transplantation into lesioned spinal cord (Lankford et al., 2008; Nazareth et al., 2015). We could hypothesize that after SCI and transplantation, OECs phagocyte axonal and myelin debris, known to strongly inhibit axonal regrowth, which may put in place a permissive microenvironment.

The precise role which is played by OECs after transplantation is difficult to characterize due to the fact that many studies have reported that the OECs survival is poor in injured spinal cords (Delarue et al., 2020; Khankan et al., 2016; Watzlawick et al., 2016). In fact, most studies have described that a very low ratio of OECs survived 2 week after SCI and transplantation and virtually no surviving cells could be found at 4 weeks (Reshamwala et al., 2019). Our bioluminescence results are in agreement with these studies. Indeed, we could not find any surviving cells 14 days after SCI and transplantation. We can hypothesize that the microenvironment which is put in place after SCI decreases OECs survival due to the release of inhibitory factors such as CSPG, myelin debris, and liberation of apoptotic factors which follow neurons and oligodendrocytes death. We and others have demonstrated that rMS can reduce apoptosis (Chalfouh et al., 2020; Dufor et al., 2019), that is why we assessed the survival rate of primary bOECs after rTSMS. Our results demonstrate that rTSMS treatment do not increase primary bOEC survival (Figure 3).

In our study, we demonstrate that rTSMS treatment modulates the spinal scar, in increasing its glial component and decreasing its fibrotic component. Moreover, our results show that rTSMS decreases inflammation and demyelination. These results confirm the data previously published by us and others (Chalfouh et al., 2020; Dufor et al., 2019). In effect, it is described that magnetic stimulation induces tissue repair after brain or spinal cord injuries (Chalfouh et al., 2020; Dufor et al., 2019). Both studies have described that one of the key roles plays by magnetic stimulation is to reduce apoptosis leading to among others neuronal survival (Chalfouh et al., 2020; Dufor et al., 2019). This specific role on apoptosis could explain why rTSMS induces "early" functional recovery. We confirm here that rTSMS treated mice show already at 15 days after SCI a statistically significant improvement of their locomotor functions (Chalfouh et al., 2020). It could also explain the positive role played by rTSMS on myelin preservation which in turn leads to neuronal survival and functional recovery. This specific role of magnetic stimulation on oligodendrocyte precursor cells (OPCs) has been already described in uninjured brain (Cullen et al., 2019). In fact, Cullen et al reported that in mice, magnetic stimulation promotes proliferation of OPCs and promotes also differentiation of OPCs to mature oligodendrocytes (Cullen et al., 2019). rTSMS plays a pleiotropic role after SCI by reducing inflammation, fibrosis, and apoptosis, which increase neuronal and oligodendroglial survival and by enhancing ependymal cells proliferation and their contribution to the lesion scar.

Altogether, the specificity of the potential roles played by both primary bOECs and rTSMS comforted us to combine these two therapies in SCI context. Surprisingly, our results show that there is no additional benefit when primary bOEC transplantation and rTSMS treatment are combined together. In effect, for all the parameters measured there is no difference between STM and primary bOECs + STM groups. Different hypotheses could be made to explain these results. The first one is that the magnetic field exert its effects on a larger spinal cord area than primary bOEC transplantation. Indeed, our magnetic coils stimulate an area of 1.5cm^2 whereas you could hypothesize that bOEC transplantation exerts their effects more locally. The second hypothesis is that rTSMS treatment and bOEC transplantation do not exert their main effects at the same time, which could explain the differences observed in locotronic test results between primary bOEC and STM groups. We can hypothesize that rTSMS, *via* reduction of apoptosis, exerts its main effects shortly after the beginning of the treatment whereas, at the opposite bOEC transplantation through neurotrophic factors secretion induces its effects at later time point. It could be of great interest to validate this hypothesis in combining rTSMS treatment, in beginning the day right after SCI and in transplanting bOECs 2 weeks later, the day after the end of rTSMS treatment. Moreover, this paradigm is more clinically relevant. Indeed, autologous OEC transplantation can be performed in Humans only after a culture step, it has been described that the necessary time to obtain the amount of cells needed for transplantation is around 12 days (Tabakow et al., 2014). Nevertheless, in our study, primary bOEC transplantation has been performed right after SCI because it has been reported that this experimental design is the most efficient one (Watzlawick et al., 2016).

In our study, primary bOECs and not purified bOECs have been transplanted due to the fact that several studies have described that the transplantation of primary bOECs is more efficient than transplantation of purified bOECs to enhance functional recovery after SCI (Watzlawick et al., 2016). Li et al have hypothesized that OB nerve fibroblasts may express regenerative properties after SCI which are linked to the specific role they play into the regeneration of the primary olfactory system (Li et al., 2005).

It is important to note that our study has been performed in female mice due to the fact that the disruption of the autonomic nervous system induces very severe urogenital complications such as necrosis of the penis due to persistent priapism. However, to our knowledge, the locomotor deficit observed after SCI are comparable between males and females (Fukutoku et al., 2020).

It could also be interesting to confirm our results in other animal models. Indeed, the cellular and molecular mechanisms which are involved after SCI are different between species. In mice the lesioned scar is mostly composed of glial and fibrotic cells without cystic cavity after contusive or penetrating injuries whereas at the opposite it is well described that in Humans after SCI large cavities are present into the lesioned spinal cord (Courtine & Sofroniew, 2019; Soderblom et al., 2013). That is why it could be of primary interest to evaluate the effects of the combination of these two therapies in an animal in which the secondary events which take place after SCI

are the same than those described in Humans such as rats or non-human primates.

DECLARATION OF TRANSPARENCY

The authors, reviewers and editors affirm that in accordance to the policies set by the *Journal of Neuroscience Research*, this manuscript presents an accurate and transparent account of the study being reported and that all critical details describing the methods and results are present.

CONFLICT OF INTEREST
The authors declare that they have no competing interests.

CONSENT FOR PUBLICATION
All authors have read the manuscript and indicated consent for publication.

AUTHOR CONTRIBUTIONS
Conceptualization, N.G.; Methodology, N.G. and Q.D.; Resources, J--P.M.; Investigation, Q.D., A.R. and R.M.; Formal Analysis, N.G. Q.D., A.R., and R.M; Writing, N.G. and Q.D - Original Draft, N.G. and Q.D.; Writing - Review & Editing, N.G. and Q.D; Supervision, N.G.; Funding Acquisition, N.G.

DATA AVAILABILITY STATEMENT
The authors confirm that the data supporting the findings of this study are available within the article and its Supporting Information.

PEER REVIEW
The peer review history for this article is available at https://publo ns.com/publo n/10.1002/jnr.24836.

ORCID
Nicolas Guérout https://orcid.org/0000-0003-0237-4981

REFERENCES
Abbaszadeh, F., Fakhri, S., & Khan, H. (2020). Targeting apoptosis and autophagy following spinal cord injury: Therapeutic approaches to polyphenols and candidate phytochemicals. *Pharmacological Research*, *160*, 105069. https://doi.org/10.1016/j.phrs.2020.105069

Ahuja, C. S., Mothe, A., Khazaei, M., Badhiwala, J. H., Gilbert, E. A., van der Kooy, D., Morshead, C. M., Tator, C., & Fehlings, M. G. (2020). The leading edge: Emerging neuroprotective and neuroregenerative cell-based therapies for spinal cord injury. *Stem Cells Translational Medicine*, *9*, 1509–1530. https://doi.org/10.1002/sctm.19-0135

Anderson, M. A., Burda, J. E., Ren, Y., Ao, Y., O'Shea, T. M., Kawaguchi, R., Coppola, G., Khakh, B. S., Deming, T. J., & Sofroniew, M. V. (2016).

Astrocyte scar formation aids central nervous system axon regeneration. *Nature*, *532*, 195–200. https://doi.org/10.1038/nature17623

Badner, A., Siddiqui, A. M., & Fehlings, M. G. (2017). Spinal cord injuries: How could cell therapy help? *Expert Opinion on Biological Therapy*, *17*, 529–541. https://doi.org/10.1080/14712598.2017.1308481

Blumenthal, J., Cohen-Matsliah, S. I., & Levenberg, S. (2013). Olfactory bulb-derived cells seeded on 3D scaffolds exhibit neurotrophic factor expression and pro-angiogenic properties. *Tissue Engineering Part A*, *19*, 2284–2291. https://doi.org/10.1089/ten.tea.2012.0090

Chalfouh, C., Guillou, C., Hardouin, J., Delarue, Q., Li, X., Duclos, C., Schapman, D., Marie, J.-P., Cosette, P., & Guérout, N. (2020). The regenerative effect of trans-spinal magnetic stimulation after spinal cord injury: Mechanisms and pathways underlying the effect. *Neurotherapeutics*, *17*, 2069–2088. https://doi.org/10.1007/s1331 1-020-00915-5

Chort, A., Alves, S., Marinello, M., Dufresnois, B., Dornbierer, J.-G., Tesson, C., Latouche, M., Baker, D. P., Barkats, M., El Hachimi, K. H., Ruberg, M., Janer, A., Stevanin, G., Brice, A., & Sittler, A. (2013). Interferon beta induces clearance of mutant ataxin 7 and improves locomotion in SCA7 knock-in mice. *Brain*, *136*, 1732–1745. https://doi.org/10.1093/brain/awt061

Courtine, G., & Sofroniew, M. V. (2019). Spinal cord repair: Advances in biology and technology. *Nature Medicine*, *25*, 898–908. https://doi.org/10.1038/s41591-019-0475-6

Cullen, C. L., Senesi, M., Tang, A. D., Clutterbuck, M. T., Auderset, L., O'Rourke, M. E., Rodger, J., & Young, K. M. (2019). Low-intensity transcranial magnetic stimulation promotes the survival and maturation of newborn oligodendrocytes in the adult mouse brain. *Glia*, *67*, 1462–1477. https://doi.org/10.1002/glia.23620

Decherchi, P., Lammari-Barreault, N., Cochard, P., Carin, M., Réga, P., Pio, J., Péllissier, J. F., Ladaique, P., Novakovitch, G., & Gauthier, P. (1997). CNS axonal regeneration within peripheral nerve grafts cryopreserved by vitrification: Cytological and functional aspects. *Cryobiology*, *34*, 214–239. https://doi.org/10.1006/cryo.1997.2003

Delarue, Q., Mayeur, A., Chalfouh, C., Honoré, A., Duclos, C., Di Giovanni, M., Li, X., Salaun, M., Dampierre, J., Vaudry, D., Marie, J.-P., & Guérout, N. (2020). Inhibition of ADAMTS-4 expression in olfactory ensheathing cells enhances recovery after transplantation within spinal cord injury. *Journal of Neurotrauma*, *37*, 507–516. https://doi.org/10.1089/neu.2019.6481

Dias, D. O., Kim, H., Holl, D., Werne Solnestam, B., Lundeberg, J., Carlén, M., Göritz, C., & Frisén, J. (2018). Reducing pericyte-derived scarring promotes recovery after spinal cord injury. *Cell*, *173*, 153–165.e22. https://doi.org/10.1016/j.cell.2018.02.004

Dufor, T., Grehl, S., Tang, A. D., Doulazmi, M., Traoré, M., Debray, N., Dubacq, C., Deng, Z.-D., Mariani, J., Lohof, A. M., & Sherrard, R. M. (2019). Neural circuit repair by low-intensity magnetic stimulation requires cellular magnetoreceptors and specific stimulation patterns. *Science Advances*, *5*, eaav9847. https://doi.org/10.1126/sciadv.aav9847

Fukutoku, T., Kumagai, G., Fujita, T., Sasaki, A., Wada, K., Liu, X., Tanaka, T., Kudo, H., Asari, T., Nikaido, Y., Ueno, S., & Ishibashi, Y. (2020, November 1). Sex-related differences in anxiety and functional recovery after spinal cord injury in mice. *Journal of Neurotrauma*, *37*(21), 2235–2243. https://doi.org/10.1089/neu.2019.6929

Göritz, C., Dias, D. O., Tomilin, N., Barbacid, M., Shupliakov, O., & Frisén, J. (2011). A pericyte origin of spinal cord scar tissue. *Science*, *333*, 238–242. https://doi.org/10.1126/science.1203165

Grégoire, C.-A., Goldenstein, B. L., Floriddia, E. M., Barnabé-Heider, F., & Fernandes, K. J. L. (2015). Endogenous neural stem cell responses to stroke and spinal cord injury. *Glia*, *63*, 1469–1482. https://doi.org/10.1002/glia.22851

Gu, M., Gao, Z., Li, X., Guo, L., Lu, T., Li, Y., & He, X. (2017). Conditioned medium of olfactory ensheathing cells promotes the functional recovery and axonal regeneration after contusive spinal cord

injury. *Brain Research*, *1654*, 43–54. https://doi.org/10.1016/j.brainres.2016.10.023

Guérout, N., Derambure, C., Drouot, L., Bon-Mardion, N., Duclos, C., Boyer, O., & Marie, J.-P. (2010). Comparative gene expression profiling of olfactory ensheathing cells from olfactory bulb and olfactory mucosa. *Glia*, *58*, 1570–1580. https://doi.org/10.1002/glia.21030

Guo, M., Wu, L., Song, Z., & Yang, B. (2020). Enhancement of neural stem cell proliferation in rats with spinal cord injury by a combination of repetitive transcranial magnetic stimulation (rTMS) and human umbilical cord blood mesenchymal stem cells (hUCB-MSCs). *Medical Science Monitor : International Medical Journal of Experimental and Clinical Research*, *26*, e924445-1–e924445-8. https://doi.org/10.12659/MSM.924445

Honoré, A., Le Corre, S., Derambure, C., Normand, R., Duclos, C., Boyer, O., Marie, J.-P., & Guérout, N. (2012). Isolation, characterization, and genetic profiling of subpopulations of olfactory ensheathing cells from the olfactory bulb. *Glia*, *60*, 404–413 https://doi.org/10.1002/glia.22274

Kanno, H., Pressman, Y., Moody, A., Berg, R., Muir, E. M., Rogers, J. H., Ozawa, H., Itoi, E., Pearse, D. D., & Bunge, M. B. (2014). Combination of engineered Schwann cell grafts to secrete neurotrophin and chondroitinase promotes axonal regeneration and locomotion after spinal cord injury. *Journal of Neuroscience*, *34*, 1838–1855. https://doi.org/10.1523/JNEUROSCI.2661-13.2014

Khankan, R. R., Griffis, K. G., Haggerty-Skeans, J. R., Zhong, H., Roy, R. R., Edgerton, V. R., & Phelps, P. E. (2016). Olfactory ensheathing cell transplantation after a complete spinal cord transection mediates neuroprotective and immunomodulatory mechanisms to facilitate regeneration. *Journal of Neuroscience*, *36*, 6269–6286. https://doi.org/10.1523/JNEUROSCI.0085-16.2016

Kucher, K., Johns, D., Maier, D., Abel, R., Badke, A., Baron, H., Thietje, R., Casha, S., Meindl, R., Gomez-Mancilla, B., Pfister, C., Rupp, R., Weidner, N., Mir, A., Schwab, M. E., & Curt, A. (2018). First-in-man intrathecal application of neurite growth-promoting anti-nogo-A antibodies in acute spinal cord injury. *Neurorehabil Neural Repair*, *32*, 578–589. https://doi.org/10.1177/1545968318776371

Lankford, K. L., Sasaki, M., Radtke, C., & Kocsis, J. D. (2008). Olfactory ensheathing cells exhibit unique migratory, phagocytic, and myelinating properties in the X-irradiated spinal cord not shared by Schwann cells. *Glia*, *56*, 1664–1678. https://doi.org/10.1002/glia.20718

Li, X., Floriddia, E. M., Toskas, K., Fernandes, K. J. L., Guérout, N., & Barnabé-Heider, F. (2016). Regenerative potential of ependymal cells for spinal cord injuries over time. *EBioMedicine*, *13*, 55–65. https://doi.org/10.1016/j.ebiom.2016.10.035

Li, Y., Field, P. M., & Raisman, G. (1997). Repair of adult rat corticospinal tract by transplants of olfactory ensheathing cells. *Science*, *277*, 2000–2002. https://doi.org/10.1126/science.277.5334.2000

Li, Y., Field, P. M., & Raisman, G. (2005). Olfactory ensheathing cells and olfactory nerve fibroblasts maintain continuous open channels for regrowth of olfactory nerve fibres. *Glia*, *52*, 245–251. https://doi.org/10.1002/glia.20241

Li, Y., He, X., Kawaguchi, R., Zhang, Y., Wang, Q., Monavarfeshani, A., Yang, Z., Chen, B., Shi, Z., Meng, H., Zhou, S., Zhu, J., Jacobi, A., Swarup, V., Popovich, P. G., Geschwind, D. H., & He, Z. (2020). Microglia-organized scar-free spinal cord repair in neonatal mice. *Nature*, *587*, 613–618. https://doi.org/10.1038/s41586-020-2795-6

Lipson, A., Widenfalk, J., Lindqvist, E., Ebendal, L., & Olson, L. (2003). Neurotrophic properties of olfactory ensheathing glia. *Experimental Neurology*, *180*, 167–171. https://doi.org/10.1016/s0014-4886(02)00058-4

López-Vales, R., Forés, J., Navarro, X., & Verdú, E. (2006). Olfactory ensheathing glia graft in combination with FK506 administration promote repair after spinal cord injury. *Neurobiology of Diseases*, *24*(3), 443–454. https://doi.org/10.1016/j.nbd.2006.08.001

López-Vales, R., Forés, J., Navarro, X., & Verdú, E. (2007). Chronic transplantation of olfactory ensheathing cells promotes partial recovery after complete spinal cord transection in the rat. *Glia*, *55*, 303–311. https://doi.org/10.1002/glia.20457

López-Vales, R., Forés, J., Verdú, E., & Navarro, X. (2006). Acute and delayed transplantation of olfactory ensheathing cells promote partial recovery after complete transection of the spinal cord. *Neurobiology of Diseases*, *21*(1), 57–68. https://doi.org/10.1016/j.nbd.2005.06.011

Mayeur, A., Duclos, C., Honoré, A., Gauberti, M., Drouot, L., do Rego, J.-C., Bon-Mardion, N., Jean, L., Vérin, E., Emery, E., Lemarchant, S., Vivien, D., Boyer, O., Marie, J.-P., & Guérout, N. (2013). Potential of olfactory ensheathing cells from different sources for spinal cord repair. *PLoS ONE*, *8*, e62860. https://doi.org/10.1371/journal.pone.0062860

Meletis, K., Barnabé-Heider, F., Carlén, M., Evergren, E., Tomilin, N., Shupliakov, O., & Frisén, J. (2008). Spinal cord injury reveals multilineage differentiation of ependymal cells. *PLoS Biology*, *6*, e182. https://doi.org/10.1371/journal.pbio.0060182

Muir, E., De Winter, F., Verhaagen, J., & Fawcett, J. (2019). Recent advances in the therapeutic uses of chondroitinase ABC. *Experimental Neurology*, *321*, 113032. https://doi.org/10.1016/j.expneurol.2019.113032

Nazareth, L., Lineburg, K. E., Chuah, M. I., Tello Velasquez, J., Chehrehasa, F., St John, J. A., & Ekberg, J. A. K. (2015). Olfactory ensheathing cells are the main phagocytic cells that remove axon debris during early development of the olfactory system. *Journal of Comparative Neurology*, *523*, 479–494. https://doi.org/10.1002/cne.23694

O'Shea, T. M., Burda, J. E., & Sofroniew, M. V. (2017). Cell biology of spinal cord injury and repair. *Journal of Clinical Investigation*, *127*, 3259–3270. https://doi.org/10.1172/JCI90608

Reshamwala, R., Shah, M., St John, J., & Ekberg, J. (2019). Survival and integration of transplanted olfactory ensheathing cells are crucial for spinal cord injury repair: Insights from the last 10 years of animal model studies. *Cell Transplantation*, *28*, 132S–159S. https://doi.org/10.1177/0963689719883823

Sabelström, H., Stenudd, M., Réu, P., Dias, D. O., Elfineh, M., Zdunek, S., Damberg, P., Göritz, C., & Frisén, J. (2013). Resident neural stem cells restrict tissue damage and neuronal loss after spinal cord injury in mice. *Science*, *342*, 637–640. https://doi.org/10.1126/science.1242576

Schneider, M. P., Sartori, A. M., Ineichen, B. V., Moors, S., Engmann, A. K., Hofer, A.-S., Weinmann, O., Kessler, T. M., & Schwab, M. E. (2019). Anti-Nogo-A antibodies as a potential causal therapy for lower urinary tract dysfunction after spinal cord injury. *Journal of Neuroscience*, *39*, 4066–4076. https://doi.org/10.1523/JNEUROSCI.3155-18.2019

Soderblom, C., Luo, X., Blumenthal, E., Bray, E., Lyapichev, K., Ramos, J., Krishnan, V., Lai-Hsu, C., Park, K. K., Tsoulfas, P., & Lee, J. K. (2013). Perivascular fibroblasts form the fibrotic scar after contusive spinal cord injury. *Journal of Neuroscience*, *33*, 13882–13887. https://doi.org/10.1523/JNEUROSCI.2524-13.2013

Stenudd, M., Sabelström, H., & Frisén, J. (2015). Role of endogenous neural stem cells in spinal cord injury and repair. *JAMA Neurology*, *72*, 235–237. https://doi.org/10.1001/jamaneurol.2014.2927

Tabakow, P., Raisman, G., Fortuna, W., Czyz, M., Huber, J., Li, D., Szewczyk, P., Okurowski, S., Miedzybrodzki, R., Czapiga, B., Salomon, B., Halon, A., Li, Y., Lipiec, J., Kulczyk, A., & Jarmundowicz, W. (2014). Functional regeneration of supraspinal connections in a patient with transected spinal cord following transplantation of bulbar olfactory ensheathing cells with peripheral nerve bridging. *Cell Transplantation*, *23*, 1631–1655. https://doi.org/10.3727/096368914X685131

Thornton, M. A., Mehta, M. D., Morad, T. T., Ingraham, K. L., Khankan, R. R., Griffis, K. G., Yeung, A. K., Zhong, H., Roy, R. R., Edgerton, V. R.,

& Phelps, P. E. (2018). Evidence of axon connectivity across a spinal cord transection in rats treated with epidural stimulation and motor training combined with olfactory ensheathing cell transplantation. *Experimental Neurology*, 309, 119–133. https://doi.org/10.1016/j.expneurol.2018.07.015

Wagner, F. B., Mignardot, J.-B., Goff-Mignardot, C. G. L., Demesmaeker, R., Komi, S., Capogrosso, M., Rowald, A., Seáñez, I., Caban, M., Pirondini, E., Vat, M., McCracken, L. A., Heimgartner, R., Fodor, I., Watrin, A., Seguin, P., Paoles, E., Keybus, K. V. D., Eberle, G., … Courtine, G. (2018). Targeted neurotechnology restores walking in humans with spinal cord injury. *Nature*, 563, 65–71. https://doi.org/10.1038/s41586-018-0649-2

Wang, G., Cheng, Z., Yuan, P., Li, H., & He, X. (2021). Olfactory ensheathing cell transplantation alters the expression of chondroitin sulfate proteoglycans and promotes axonal regeneration after spinal cord injury. *Neural Regeneration Research*, 16, 1638–1644. https://doi.org/10.4103/1673-5374.301023

Watzlawick, R., Rind, J., Sena, E. S., Brommer, B., Zhang, T., Kopp, M. A., Dirnagl, U., Macleod, M. R., Howells, D. W., & Schwab, J. M. (2016). Olfactory ensheathing cell transplantation in experimental spinal cord injury: Effect size and reporting bias of 62 experimental treatments. *A Systematic Review and Meta-Analysis*, 14, e1002468. https://doi.org/10.1371/journal.pbio.1002468

Zhang, L., Zhuang, X., Kotitalo, P., Keller, T., Krzyczmonik, A., Haaparanta-Solin, M., Solin, O., Forsback, S., Grönroos, T. J., Han, C., López-Picón, F. R., & Xia, H. (2021). Intravenous transplantation of olfactory ensheathing cells reduces neuroinflammation after spinal cord injury via interleukin-1 receptor antagonist. *Theranostics*, 11, 1147–1161. https://doi.org/10.7150/thno.52197

SUPPORTING INFORMATION

Additional Supporting Information may be found online in the Supporting Information section.

Transparent Science Questionnaire for Authors

Supplementary Material

How to cite this article: Delarue Q, Robac A, Massardier R, Marie J-P, Guérout N. Comparison of the effects of two therapeutic strategies based on olfactory ensheathing cell transplantation and repetitive magnetic stimulation after spinal cord injury in female mice. *J Neurosci Res*. 2021;99:1835–1849. https://doi.org/10.1002/jnr.24836